Available online at www.sciencedirect.com
SCIENCE DIRECT
Cement and Concrete Research 35 (2005) 2364 – 2370
Cement and Concrete Research

Role of disjoining pressure in cement based materials

Françoise Beltzung[a,*], Folker H. Wittmann[a,b]

[a]Aedificat Institute, 79110 Freiburg, Germany
[b]Qingdao University of Technology, Qingdao, China

Received 20 September 2004; accepted 6 April 2005

Abstract

During the hydration process of Portland cement a nanoporous gel is formed. The high internal surface of the hydration products, mainly calcium-silicate hydrates, and the numerous adsorbed cations interact with water. At an equilibrium moisture content below 50% adsorbed water molecules reduce the surface tension of the solid particles. Water adsorbed at higher relative humidity is at the origin of disjoining pressure acting in small gaps between particles. Both processes are major mechanisms of shrinkage and swelling of hardened cement paste. Results of investigations into the disjoining pressure are summarised. The relevance of disjoining pressure for the behaviour of cement-based materials will be discussed.

Keywords: Shrinkage; Pore solution; Surface layer; Disjoining pressure; Calcium-silicate hydrate

1. Introduction

It is generally admitted that four major mechanisms are involved in the drying shrinkage or wetting swelling of cementitious materials. For relative humidities below 50% hygral volume changes are mainly due to the Bangham's law [1] which describes the relationship between the macroscopic length change and the change of surface tension of an adsorbent. Practically, this means for hardened cement paste that when the relative humidity of the environment of hydration products is increased, water molecules are gradually adsorbed, surface tension decreases [2] and, consequently, the nanoparticles expand [3,4].

At relative humidities above 50% the interaction is getting more complex and the interpretation of results remains controversial until now. Both capillary and disjoining forces are assumed to act in combination so as to fulfil the equilibrium of mechanical forces and equality of the chemical potentials [5]:

$$P_c - \Pi = -(RT/v_m)\cdot\ln(p/p_s) \quad (1)$$

where P_c is the capillary underpressure, Π is the disjoining pressure, v_m is the molar volume of the liquid and p_s is its saturation vapour pressure.

The first open question concerns the lower limit of validity of the Laplace equation. Two limiting effects are to be considered at least. The water within the range of surface forces (physically adsorbed water) and the structured water surrounding the cations is significantly different from bulk water. Therefore, the simple model of a regular (spherical) shaped meniscus with the contact angle close to zero is questionable at low relative humidities. Furthermore, in pores containing bulk water, the macroscopic liquid–vapour surface tension ought to be corrected in order to allow for the discrete structure of water at nanometer scale.

The second open question concerns the magnitude of the disjoining pressure which develops in a cement based material. Based on findings of several authors one can conclude that disjoining pressure is of the order of magnitude of 1 MPa. But higher values have also been observed. Churaev and Sobolev [6] have determined disjoining pressures of non freezing films as large as 8 MPa, and Pashley and Kitchener [7] measured values up to 15 MPa on quartz systems. In parallel, the swelling

* Corresponding author. Fax: +41 61 467 46 10.
E-mail address: f.beltzung@fhbb.ch (F. Beltzung).

0008-8846/$ - see front matter © 2005 Elsevier Ltd. All rights reserved.
doi:10.1016/j.cemconres.2005.04.004

pressure of clays has been determined experimentally in different types of geotechnical test set-ups such as oedometer and triaxial cells. The values measured on bentonite for instance vary between 10^3 and 10^8 Pa according to [8] or between 3 MPa (at 95% RH) and 50 MPa (at 45% RH) according to [9].

These questions are obviously crucial if one wants to determine the relative humidity above which the system may be supposed to experience a dominant capillary underpressure. Fig. 1 shows a precise length change isotherm as measured on cement paste by Feldman [10]. At low relative humidities, say HR<50%, one or two molecular layers of water are built up and the expansion finds its origin in the Bangham effect [1,3,4] and in the decrease of the van der Waals attraction in the region of 0%<RH<30% [3,11]. Additional swelling occurs because water molecules are gradually incorporated between the layers of the C–S–H particles. At RH>50%, up to five water layers cover the surfaces of the pores and at least two water layers surround cations [12]. As soon as opposite water layers and hydration shells join within the smallest nanopores ($1<r<3$ nm) structural forces move the C–S–H particles apart until equilibrium between actual water vapour and structured water is reached. Thus when finally capillary condensation of bulk water occurs the relative humidity may be expected to be as high as 90%, or even higher.

Based on values of P_c calculated by means of the Laplace equation and comparing these values with the much lower measured or calculated values of Π, shrinkage should be observed as soon as the point of capillary condensation is reached. The isotherm (Fig. 1) just as other published data show, however, that considerable expansion occurs in the whole range of increasing relative humidities.

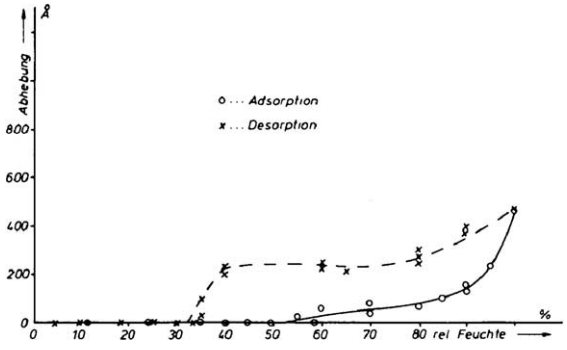

Fig. 2. Gap height between two flat quartz surfaces versus RH (after Splittgerber [13]).

The main objective of this paper is to investigate and discuss the nature of dominant phenomena of shrinkage. It is common to assume that volume changes of hardened cement paste above 50% RH are controlled by capillary forces exclusively. There is indeed no doubt that one driving force of hygral shrinkage is the decrease of the radius of menisci if capillary water is present. But, on the other hand, the observed value of shrinkage must be the resultant of the

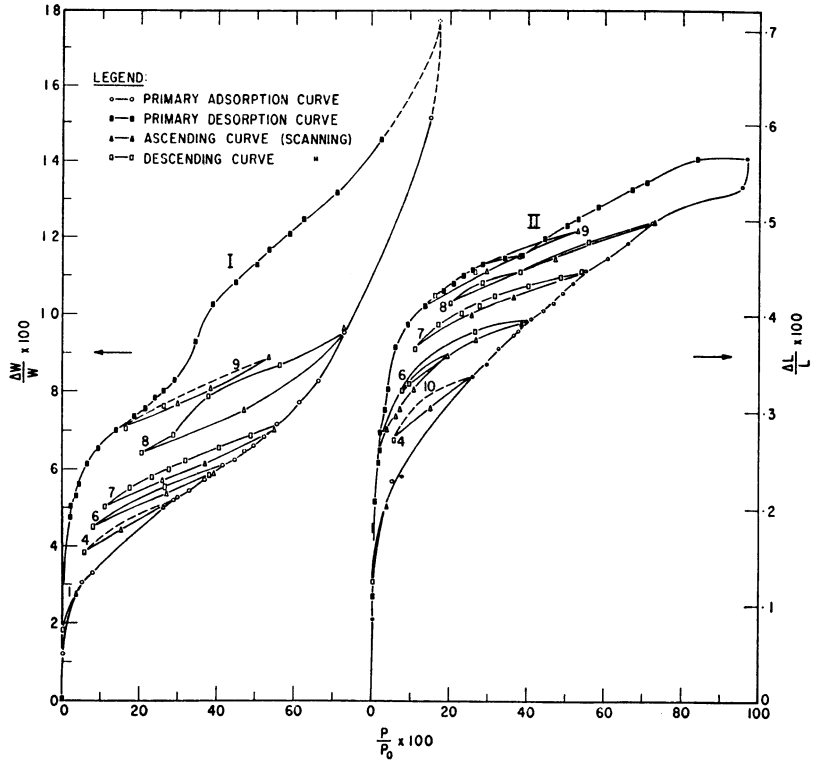

Fig. 1. Weight change (I) and hygral length change (II) isotherms of hardened cement paste, w/c=0.5 (after Feldman [10]).

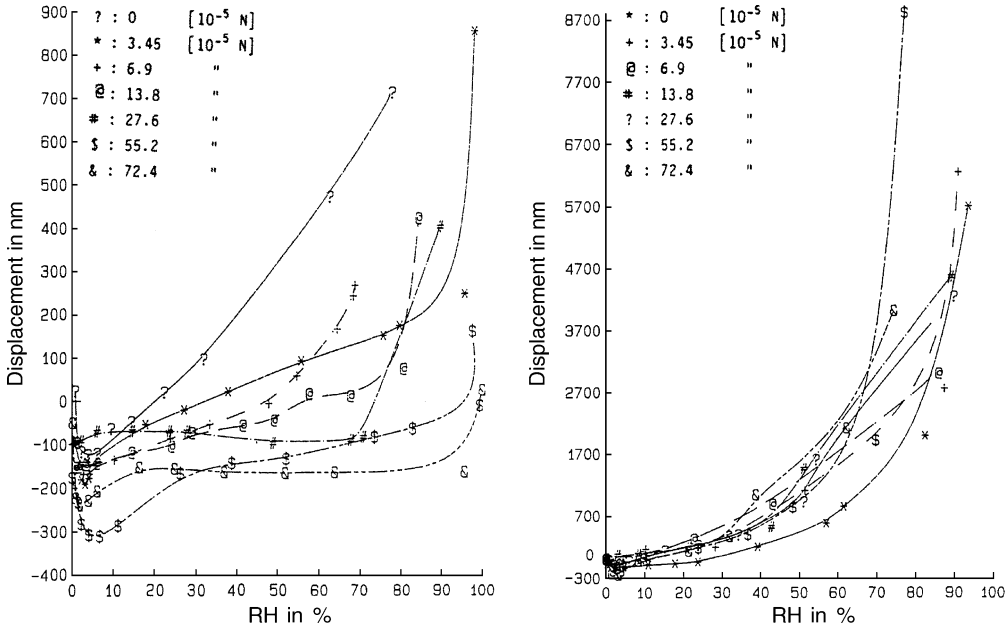

Fig. 3. Displacement between two spherical surfaces versus RH; the curves differentiate with the force applied (after Ferraris [14]). Left: quartz surfaces. Right: mica surfaces.

joint action of capillary underpressure and disjoining pressure since both are involved in establishing thermodynamical and mechanical equilibrium.

2. Results

2.1. Surface separation experiments

The action of disjoining pressure has already been evidenced by numerous experiments. The length change isotherm as shown in Fig. 1 suggests that disjoining forces dominate the macroscopic swelling of a nanoporous material in the range RH>50%. This statement is further verified by results obtained from experiments on surfaces initially in contact. These comparatively simple systems allow to measure separations of two opposing surfaces at nm scale. Again, none of the published surface separation versus RH diagrams show, at higher relative humidities, any discontinuity which could suggest the possible existence of dominating attractive forces. This fact is illustrated by results found independently by Splittgerber [13] (Fig. 2) and Ferraris [14] (Fig. 3).

We have developed a simple mechanical device to measure the action of disjoining pressure. Essential parts are shown schematically in Fig. 4. Typical results are shown in Fig. 5.

2.2. Influence of cation concentration

The disjoining pressure as measured with surface force apparatuses on mica, quartz or glass systems shows a pronounced dependence on the nature and bulk concentration of dissolved cations [15,16,17]. This effect is inter-

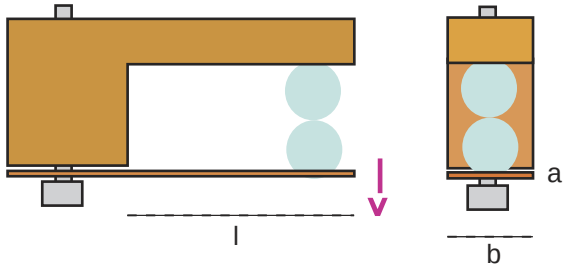

Fig. 4. Experimental set-up for observation of disjoining force between two quartz spheres; the dimensions of the brass lamella are: $a=0.06$ mm, $b=2.0$ mm and $l=6.0$ mm; the lamella is acting as a spring; thus, due to changing humidity conditions, spheres are allowed to move apart and back; the phenomenon has been investigated with ESEM.

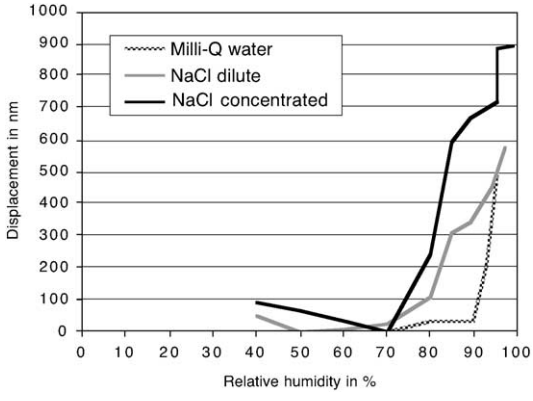

Fig. 5. Separation distance between two quartz spheres as a function of RH and NaCl concentration. The experimental set-up is shown in Fig. 4.

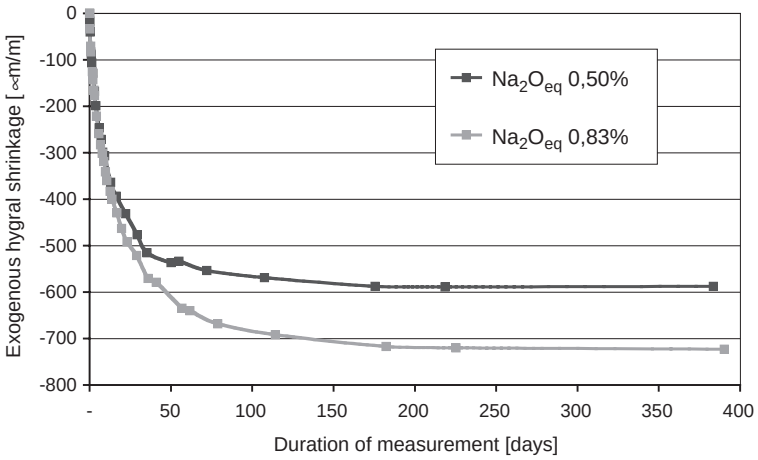

Fig. 6. Exogenous hygral shrinkage of 0/16 concrete as a function of time and natural alkali content (Na_2O_{eq}) of cement; w/c=0.40.

preted as a manifestation of ion hydration and its influence on disjoining pressure. Similarly, results from clay swelling and from hardened cement paste shrinkage experiments suggest that the valency and ion concentration are of decisive importance.

The global dependence of surface separation on NaCl concentration has been clearly outlined by the results shown in Fig. 5. However, the simplicity of the experimental device and the complicated nature of disjoining pressure, which is the sum of at least three components, make any quantitative interpretation difficult. Shrinkage measurements on concrete and mortar made with natural or alkali enriched cements indicate that a change in the composition of pore solution influences the hygral deformation. Shrinkage data of concrete mixed with selected cements having different natural alkali contents suggest that alkaline oxides promote hygral shrinkage. A typical example is presented in Fig. 6.

The latter observation has been confirmed by alkali enrichment of mortars by adding sodium or potassium hydroxide to the mixing water. Three enrichment series are described in Tables 1 and 2. Reference mortars are referred to as LT1 and WE1. Mix proportions are the same for all mortar specimens. Water-to-cement ratio and sand-to-cement ratio are 0.40 and 1.44, respectively. A typical series of results is shown in Fig. 7. Moreover, 200 days data have been extrapolated to ultimate shrinkage at $t\rightarrow\infty$ for each curve. The graph in Fig. 8 shows the relationship between the total amount of alkali oxide and the ultimate hygral shrinkage. This figure summarizes results of the whole campaign.

3. Discussion of the results

3.1. Surface separation as a function of relative humidity

Evidence for the existence of repulsive forces and for the influence of dissolved ions on the interaction between solid surfaces and a liquid is provided by data shown in Fig. 5. Two quartz spheres with a radius of 1 mm, in contact in the dry state, are moving apart from each other when the relative humidity is increased and hence water is adsorbed and capillary condensed. When surfaces are clean (marked with Milli-Q water) the spheres adhere up to 70% RH, then they move slightly apart up to 90% and finally, close to saturation, the spreading reaches 500 nm. This result is very similar to the one obtained by Ferraris [14]. According to Fisher [18], Deryagin and Churaev [19] and Pashley and Kitchener [7], several structured water layers can adsorb on quartz. Below 90%, the resulting film thickness remains small but above 90% it diverges and allows a sharp separation motion by disjoining pressure.

By adding monovalent salts spreading is amplified and starts at a RH as low as 60–70%. Thus, there is clear evidence that dissolved ions contribute considerably to disjoining pressure, either by DLVO repulsion or by ion hydration.

Fig. 3 shows results from a previous experiment by Ferraris [14] carried out on both quartz and mica surfaces. Mica separation increases continuously and exceeds by one order of magnitude the more erratic quartz separation. This distinct behaviour is in good agreement with the cation exchange capacity of the two materials. This reaction is negligible for quartz. Mica contains exchangeable cations

Table 1
Alkali oxide enrichment of Portland cement LT

	LT1	LT2	LT3	LT4	LT5	LT6	LT7	LT8
Na_2O	0.19	0.40	0.80	1.00	1.20	0.19	0.19	0.19
K_2O	0.25	0.25	0.25	0.25	0.25	0.40	0.80	1.00

Table 2
Sodium oxide enrichment of Portland cement WE

	WE1	WE2	WE3	WE4
Na_2O	0.0	0.4	0.8	1.0
K_2O	1.1	1.1	1.1	1.1.

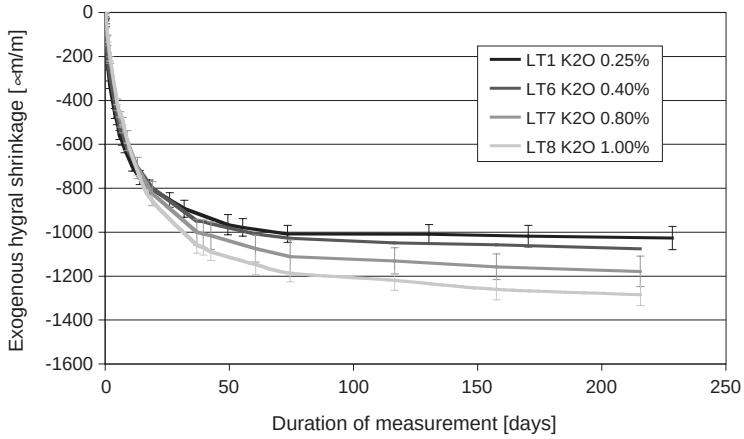

Fig. 7. Drying shrinkage measurement at 60% RH and 20 °C; measurements have been started 1 week after mixing; mortar's mix proportions are w/c = 0.40 and s/c = 1.44; LT1 is the mean curve obtained with reference samples whereas LT6, LT7 and LT8 are obtained with mortars that have been enriched in potassium oxide; the total amount is indicated in % by weight of cement (see Table 1).

which dissolve within the adsorbed liquid layer. Thus additional disjoining forces are generated by the hydration of ions and/or by the electrical double layer which builds up.

These general observations allow us to conclude that, in the systems considered here, disjoining pressure exceeds capillary underpressure and therefore it controls essentially hygral volume change as a function of RH. Furthermore, whenever electrolytes are present, repulsive forces become even more pronounced and lead to surface separation process. This statement is in obvious contradiction with the assumption of capillary underpressure calculated according to the Laplace equation being a decisive mechanism of shrinkage or swelling of cement-based materials. Therefore, two hypothesis are conceivable. Either capillary underpressure is overestimated or it is not operating as expected.

3.2. Capillary pressure at the scale of a few nanometers

Based on their experiments carried out on capillary forces, Fisher [18], Crassous et al. [20] and Schubert [21] do not agree in all details but they all accept the limiting effect of the thickness of the anisotropic liquid–vapour transition layer. The following equation predicts the actual surface tension γ as a function of the mean meniscus radius r_m [18,21]:

$$\gamma = \gamma_\infty(1 - 2\delta/r_m) \quad (2)$$

where γ_∞ is the macroscopic surface tension and δ is the thickness of the liquid/vapour interface, estimated for water to be one layer of 0.3 nm [21]. Eq. (2) implies that the capillary pressure which occurs at very small dimensions of the meniscus is much smaller than predicted by the macroscopic Laplace equation. Figs. 9 and 10, respectively, show the calculated capillary underpressure and Kelvin radius according to $\gamma = \gamma_\infty$ and $\gamma = \gamma_\infty(1 - 0.6/r_m)$.

This scale dependent limitation of the Laplace equation is valid for all curved liquid/vapor interfaces. In some solid/liquid/vapor systems, however, additional features have to be taken into account. This is typically the case for smectite clays and by analogy for hydrated cement paste in presence of water vapor. The nanopores of these

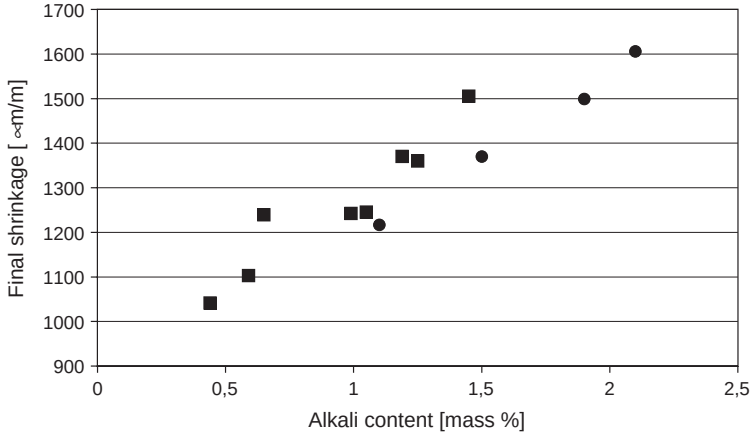

Fig. 8. Extrapolated final exogenous drying shrinkage as a function of total alkali oxide % by weight (see Tables 1 and 2); cements LT and WE are distinguished by squares and circles, respectively.

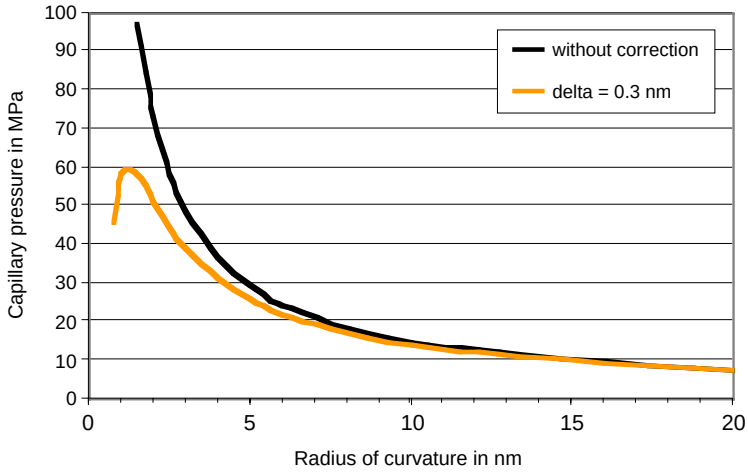

Fig. 9. Capillary pressure ΔP according to Laplace: $\Delta P=2\gamma/r_m$. Surface tension γ has been corrected in order to allow for the discrete structure of water at nanometer scale: $\gamma=\gamma_\infty(1-2\delta/r_m)$. The thickness δ of the water–vapour transition layer corresponds to one molecular diameter, i.e. 0.3 nm.

solids are not principally filled with capillary condensate but with several layers of adsorbed water due to the hydrophilicity of their surfaces. Furthermore, a high surface charge density is partially compensated by the adsorption of dissolved cations each of them being surrounded by a hydration shell. As a consequence the water/vapor interface is not comparable to a capillary meniscus and the validity of Laplace equation in this range is all the more questionable.

Since the nanopores of C–S–H are primarily filled with structured water, capillary underpressure is negligible and the principal mechanism involved in hygral shrinkage or swelling is of colloidal nature, namely disjoining pressure.

3.3. Role of alkali cations in gel pores

In anhydrous cement alkalis are present either as impurities in C_3A and C_2S or as sulphate. After mixing cement and water K_2SO_4 is readily soluble while Na_2O is released as hydration proceeds. The following substitution takes place

$$Ca(OH)_2 + K_2SO_4 + 2H_2O \Leftrightarrow CaSO_4{\cdot}2H_2O + 2KOH \quad (3)$$

which produces secondary gypsum and increases the pH of the pore solution.

Moreover, according to the solubility product of portlandite

$$[Ca^{2+}][OH^-]^2 = K_p \quad (4)$$

an increase in KOH and NaOH concentration induces a decrease of $Ca(OH)_2$ solubility. The negatively charged surfaces of the hydration products adsorb preferentially the Ca^{2+}, K^+ and Na^+ cations. A hydration shell of at least two molecular layers surrounds the cations. The gap width between two neighbouring C–S–H surfaces growing into the pore solution depends on the volume of structured water which covers each surface. This volume consists of adsorbed water films (±5 molecular layers) and hydration shells. The gap width becomes all the more important as the available cations become more numerous.

When in the course of desiccation structured water evaporates, disjoining pressure is reduced and due to attractive forces the surfaces come closer. Macroscopic shrinkage deformation occurs. Since the relative distance of two opposite surfaces is proportional to the amount of structured water lying between them, it may be assumed that alkali concentration in the pore solution influences hygral shrinkage of hardened cement paste. Experimental results shown in Figs. 6, 7 and 8 illustrate this clearly.

The attractive forces mentioned in the previous section are van der Waals and ion–ion correlation forces. The latter has first been modelled by Kjellander et al. [22] as a deviation of the classical Poisson-Boltzmann theory. The ion–ion correlation force is only significant at high surface charge densities and in the presence of bi- or trivalent ions. Later, Lesko et al. [23] have been able to confirm the accuracy of the model by

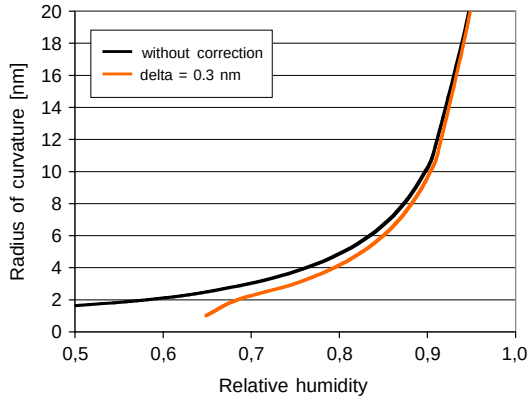

Fig. 10. Kelvin radius of curvature according to Laplace: $\Delta P=2\gamma/r_m$. Surface tension γ has been corrected in order to allow for the discrete structure of water at nanometer scale: $\gamma=\gamma_\infty(1-2\delta/r_m)$. The thickness δ of the water–vapour transition layer corresponds to one molecular diameter, i.e. 0.3 nm.

AFM measurements on C–S–H. Further, it should be mentioned that van Damme [24] attributes the cohesion and therefore the mechanical strength of cementitious materials to the Ca–Ca correlation. From this it may be inferred that the hygral deformation potential of the C–S–H structure is all the more important as the Ca^{2+} concentration of the pore solution is high. As the solubility of $Ca(OH)_2$ is inversely proportional to the alkali concentration (Eq. (4)), cements with high alkali content lead to a C–S–H structure which is more deformable. Both effects, i.e. a higher volume of structured water and a lowered cohesion, lead to more hygral shrinkage at high alkali concentration.

4. Conclusions

The following conclusions can be drawn from results compiled in this contribution:

- Equilibrium hygral length change increases steadily with increasing relative humidity.
- Hygral expansion above 50% RH is explained by the fact that disjoining pressure is clearly the dominant mechanism since the pore solution at a scale of a few nanometers cannot form a capillary meniscus.
- Na^+ and K^+ content of the pore solution influences disjoining pressure and as a consequence hygral length change.
- Shrinkage may be significantly reduced by optimizing the chemical composition of the pore solution.
- Further research is needed to fully understand the complex interaction between hydration products and the pore solution.

References

[1] D.H. Bangham, N. Fakhoury, A.F. Mohamed, The swelling of charcoal Part: III Experiments with the lower alcohols, Proc. R. Soc., A 147 (1934) 152–171.
[2] J. Adolphs, Inverse Gaschromatographie an Zementstein bei unterschiedlicher Feuchte, Abschlussbericht Teil Deutsche Forschungsgemeinschaft, Projektförderung DFG AD 144 /4 1–3 (2002).
[3] F.H. Wittmann, Grundlagen eines Modells zur Beschreibung charakteristischer Eigenschaften des Betons, Schriftenreihe Deutscher Ausschuss für Stahlbeton 290 (1977) 43–101.
[4] M.J. Setzer, Einfluss des Wassergehaltes auf die Eingenschaften des erhärteten Betons, Schriftenreihe Deutscher Ausschuss für Stahlbeton 280 (1977).
[5] N.V. Churaev, J. Adolphs, The influence of wetting films on capillary condensation in model capillary-porous bodies, Coll. J. 62 (2000) 495–498.
[6] N.V. Churaev, V.D. Sobolev, Disjoining pressure of water films in frozen materials, Rilem Proceedings 24 on Frost Resistance of Concrete, 2002, pp. 97–103.
[7] R.M. Pashley, J.A. Kitchener, Surface forces in adsorbed multilayers of water on quartz, J. Colloid Interface Sci. 71 (1979) 491–500.
[8] O. Karnland, Bentonite swelling pressure in strong NaCl solutions, SKB Technical Report 97-31, Swedish Nuclear Fuel and Waste Management Company, Stockholm, 1997.
[9] G. Kahr, et al., Wasseraufnahme und Wasserbewegung in Hochverdichtetem Bentonit, Nagra Technischer Bericht 86-14, Baden, Switzerland, 1986.
[10] R.F. Feldman, Sorption and length—change scanning isotherms of methanol and water on hydrated portland cement, Proceedings Symp. Chem. of Cement, Tokyo, vol. 3, 1968, pp. 53–66.
[11] H. Splittgerber, F.H. Wittmann, Einfluβ adsorbierter Wasserfilme auf die van der Waals Kraft zwischen Quarzglasoberflächen, Surf. Sci. 41 (1974) 504–514.
[12] K. Jasmund, G. Lagaly, Tonminerale und Tone, Steinkopff Verlag, 1993.
[13] H. Splittgerber, Spaltdruck zwischen Festkörpern und Auswirkung auf Probleme in der Technik, Cem. Concr. Res. 6 (1976) 29–36.
[14] C.F. Ferraris, Mécanismes du retrait de la pâte de ciment durcie, Thesis n° 621, Swiss Institute of Technologie, Lausanne, 1986.
[15] R.M. Pashley, DLVO and hydration forces between mica surfaces in Li^+Na^+, K^+ and Cs^+ electrolyte solutions, J. Colloid Interface Sci. 83 (1981) 531–546.
[16] N.V. Churaev, M.J. Setzer, O. Wowra, M. Reick, Electrolytes in narrow pores, Int. Z. für Bauinstand-setzen und Baudenkmalpflege 6 Heft 1 (2000) 87–102.
[17] G. Peschel, P. Belouschek, M.M. Müller, M.R. Müller, R. König, The interaction of solid surfaces in aqueous systems, Colloid Polym. Sci. 260 (1982) 444–451.
[18] L.R. Fisher, Forces due to capillary-condensed liquids: limits of calculations from thermodynamics, Adv. Colloid Interface. Sci. 16 (1982) 117–125.
[19] B.V. Deryagin, N.V. Churaev, Structure of water in thin layers, Langmuir 3 (1987) 607–612.
[20] J. Crassous, E. Charlaix, H. Gayvallet, J.-L. Loubet, Experimental study of a nanometric liquid bridge with a surface force apparatus, Langmuir 9 (1993) 1995–1998.
[21] H. Schubert, Kapillarität in Porösen Feststoffsystemen, Springer-Verlag, 1992.
[22] R. Kjellander, S. Marcelja, J.P. Quirk, Attractive double-layer interactions between calcium clay particles, J. Colloid Interface Sci. 126 (1988) 194–211.
[23] S. Lesko, E. Lesniewska, A. Nonat, J.-C. Mutin, J.-P. Goudonnet, Investigation by atomic force microscopy of forces at the origin of cement cohesion, Ultramicroscopy 86 (2001) 11–21.
[24] H. van Damme, Colloidal chemo-mechanics of cement hydrates and smectite clays: cohesion vs. swelling, Encyclopedia of Surface and Colloid Science, Marcel Decker Inc., New York, 2002, pp. 1087–1103.